Reaction dynamics in double ionization of helium by electron impact

M. F. Ciappina*
Institute of High Performance Computing, 1 Fusionopolis Way, 16-16 Connexis, 138632 Singapore

M. Schulz
Department of Physics and Laboratory for Atomic, Molecular and Optical Research, Missouri University of Science & Technology, Rolla, Missouri 65409, USA

T. Kirchner
Department of Physics and Astronomy, York University, 4700 Keele Street, Toronto, Ontario, Canada M3J 1P3
(Received 28 October 2010; published 1 December 2010)

We present theoretical fully differential cross sections (FDCS) for double ionization of helium by 500 eV and 2 keV electron impact. Contributions from various reaction mechanisms to the FDCS were calculated separately and compared to experimental data. Our theoretical methods are based on the first Born approximation. Higher-order effects are incorporated using the Monte Carlo event generator technique. Earlier, we successfully applied this approach to double ionization by ion impact, and in the work reported here it is extended to electron impact. We demonstrate that at 500 eV impact energy, double ionization is dominated by higher-order mechanisms. Even at 2 keV, double ionization does not predominantly proceed through a pure first-order process.

DOI: 10.1103/PhysRevA.82.062701 PACS number(s): 34.80.Dp, 34.10.+x, 34.50.Fa

I. INTRODUCTION

Double ionization of atoms by charged-particle impact continues to attract considerable interest largely because of the important role electron-electron correlations are known to play in this two-electron process (e.g., [1–18]). However, both experimental and theoretical studies tend to be much more challenging than for one-electron processes like single ionization. From a theoretical perspective it is the inclusion of electron-electron correlations that makes the calculations difficult. Experimentally, the main difficulty is the generally very small cross section, which makes measurements increasingly difficult with increasing degree of differentiality of the cross sections under investigation. Only two groups have reported fully differential data for electron impact [4–7]; and for ion impact, only one nearly fully differential data set is currently available [8]. Because of these difficulties even a qualitative understanding of the double-ionization dynamics is just starting to emerge.

Until recently, double ionization was often discussed in terms of two mechanisms [1]. In one, dubbed the two-step-1 projectile-electron interaction (TS-1), the projectile interacts with only one electron directly. The second electron is then ejected through correlation with the first electron. Closely related to this mechanism is the so-called shake-off process, which also only involves one direct projectile-electron interaction. Here, the second electron is ejected through a rearrangement process in the target ion induced by the change of the target Hamiltonian due to the ejection of the first electron. For simplicity, we use the label TS-1 for both of these first-order processes, both of which require the presence of electron-electron correlations. In the second mechanism the electrons are ejected in two independent interactions of the projectile with both electrons. Here, electron-electron correlations may be present, but are not required for double ionization to take place. This second (or higher)-order process is known as two-step-2 projectile-electron interactions (TS-2). Until recently, TS-1 was believed to dominate double ionization for collision systems with small perturbation parameters η (projectile charge to speed ratio), while TS-2 was thought to be the main contributor at large η (e.g., [1]). Our recent studies, based on a combination of two new and very powerful data analysis tools, suggest that these assumptions may have to be somewhat modified. In the first analysis tool, called the Monte Carlo event generator (MCEG) technique, theoretical fully differential cross sections are converted to an event file containing the momentum components of all collision fragments for a large number of simulated double-ionization (or any other process) events [19–21]. The second tool is used to generate four-particle Dalitz (4-D) plots. In these spectra, the relative squared momenta of the four collision fragments are represented simultaneously in a single plot using a tetrahedral coordinate system [22]. Using conventional methods it is extremely difficult (if not impossible) to calculate 4-D plots because they possess only a low degree (if any) of symmetry that theory could take advantage of to reduce the dimension of the numeric integration required in the calculation. However, once a theoretical event file is generated using the MCEG technique it is straightforward to extract 4-D plots exactly the same way as is done in the experimental data analysis.

We have recently reported detailed comparisons between experimental and theoretical 4-D plots for double ionization of helium in collisions with a variety of different ionic projectiles [16–18]. These studies revealed that for fast proton impact, double ionization is not dominated by TS-1, as assumed previously, but rather higher-order contributions do play an important role [16]. More recent work, studying multiple differential angular distributions of the ejected electrons in addition to the 4-D plots, then demonstrated that TS-2 is not the dominant double-ionization mechanism, either. Instead, the experimental data could be nicely reproduced by a calculation which was based on a new double-ionization channel labeled

*Present address: ICFO-Institut de Ciènces Fotòniques, 08860 Castelldefels (Barcelona), Spain.

TS-1-elastic scattering (TS-1-EL) [17]. This mechanism is perhaps best viewed as a hybrid process between TS-1 and TS-2: it bears significant resemblance to TS-1 in that here, too, only one electron is ejected by a direct interaction with the projectile and the second electron through correlation with the first electron. But it also bears significant resemblance to TS-2 in that the projectile nevertheless undergoes an interaction with the second electron as well, but only after this electron was already ejected to the continuum (i.e., this last step represents elastic scattering). Finally, for highly charged ion impact, corresponding to large η, the comparison between experiment and theory showed a predominance of TS-2, as expected [18].

The motivation for the work presented in this article was to test our theoretical models further by applying them to other collision systems. The availability of multiple differential data for ion impact is rather limited. On the other hand, more extensive literature exists for electron impact. No measured 4-D plots have been reported yet for this case, but several data sets on fully differential cross sections (FDCS) are available [4–7]. Here we report calculated FDCS for double ionization by 500 eV and 2 keV electron impact.

II. THEORETICAL FRAMEWORK

As stated in the Introduction, electron (and ion) impact double ionization (DI) can be analyzed in terms of different mechanisms. Consequently, our theoretical approaches are based on this separation. Possible interference between various scattering amplitudes is thus not accounted for in our models. In this section, we first explain how we account for the TS-1 mechanism and then describe briefly our models for the higher-order processes (TS-1-EL and TS-2).

A. FDCS for electron impact in the first Born approximation

We calculate DI cross sections differential in the momenta of the two ejected electrons $\mathbf{k}_1$ and $\mathbf{k}_2$ and in the transverse component $\mathbf{q}_\perp$ of the momentum transfer $\mathbf{q} = \mathbf{k}_0 - \mathbf{k}_f = \mathbf{q}_\perp + q_z\hat{\mathbf{k}}_\mathbf{0}$, where $\mathbf{k}_0$ and $\mathbf{k}_f$ are the initial and final momenta of the projectile and $\mathbf{q}_\perp \cdot \hat{\mathbf{k}}_\mathbf{0} = 0$ with $\hat{\mathbf{k}}_\mathbf{0}$ being the direction of $\mathbf{k}_0$. Since we are interested in electron collisions at relatively high energies, we can employ the relationship $q_z = \Delta\epsilon/k_f$, where the projectile energy loss is given by $\Delta\epsilon = k_1^2/2 + k_2^2/2 + |\varepsilon_i|$ with ε_i being the total binding energy of the helium atom.

The FDCS can be written as

$$\frac{d^8\sigma}{d\mathbf{k}_1 d\mathbf{k}_2 d\mathbf{q}_\perp} = \frac{(2\pi)^4}{k_0^2}|T_{if}|^2, \tag{1}$$

where we have reduced the dimensionality using the energy conservation δ-function $\delta(E_i - E_f)$, E_i (E_f) being the total initial (final) energy of the system. The first-order transition amplitude T_{if} is given as (see, e.g., [23])

$$T_{if} = \langle \Psi_f^{(-)}|\hat{V}|\Psi_0\rangle, \tag{2}$$

with the initial (final) state wave function Ψ_0 ($\Psi_f^{(-)}$) and the perturbation $\hat{V}$, which consists of the Coulomb interactions between the incoming projectile electron and all the constituents of the helium atom, i.e., both electrons and the nucleus.

Within the first Born approximation (FBA) a nonzero DI amplitude is obtained only if electron-electron correlations are taken into account in the initial and final states of the system. The full initial state Ψ_0 is approximated by a simple product of a plane wave for the incoming electron $\Psi_{\mathbf{k}_0}$ and a two-electron wave function ϕ_0 that represents the helium ground state, i.e., exchange between the projectile and target electrons is assumed to be negligible in the impact energy region of interest

$$|\Psi_0\rangle = \left|\Psi_{\mathbf{k}_0}\right\rangle|\phi_0\rangle. \tag{3}$$

The He ground-state wave function is taken as a symmetrized product of hydrogenlike $1s$ orbitals

$$\phi_0(\mathbf{r}_1,\mathbf{r}_2) = N(e^{-Z_a r_1}e^{-Z_b r_2} + e^{-Z_b r_1}e^{-Z_a r_2}), \tag{4}$$

with effective charges Z_a and Z_b which are found variationally as $Z_a = 2.183\,171$ and $Z_b = 1.188\,530$. This model yields a ground-state energy of $\varepsilon_i = -2.8757$ a.u. [24], which is below the Hartree-Fock result $\varepsilon_i = -2.8617$ a.u. for the $1s^2$ configuration. This suggests that radial correlation is included to some extent.

The final-state wave function of the system is written as

$$|\Psi_f^-\rangle = \left|\Psi_{\mathbf{k}_f}\right\rangle\left|\phi_{\mathbf{k}_1,\mathbf{k}_2}^{(-)}\right\rangle, \tag{5}$$

where $\Psi_{\mathbf{k}_f}$ represents a plane wave for the (fast) outgoing projectile and $\phi_{\mathbf{k}_1,\mathbf{k}_2}^{(-)}$ is a two-electron continuum state for the (slow) ejected electrons. Within the FBA the integral over the projectile coordinate can be calculated analytically. One finds

$$T_{if} = \frac{-1}{2\pi^2 q^2}[Z_T M_0 - M_1 - M_2], \tag{6}$$

with the target nuclear charge $Z_T = 2$ and

$$M_0 = \int d\mathbf{r}_1 \int d\mathbf{r}_2 \phi_{\mathbf{k}_1,\mathbf{k}_2}^{(-)*}(\mathbf{r}_1,\mathbf{r}_2)\phi_0(\mathbf{r}_1,\mathbf{r}_2), \tag{7}$$

$$M_1 = \int d\mathbf{r}_1 \int d\mathbf{r}_2 \phi_{\mathbf{k}_1,\mathbf{k}_2}^{(-)*}(\mathbf{r}_1,\mathbf{r}_2)e^{i\mathbf{q}\cdot\mathbf{r}_1}\phi_0(\mathbf{r}_1,\mathbf{r}_2), \tag{8}$$

$$M_2 = \int d\mathbf{r}_1 \int d\mathbf{r}_2 \phi_{\mathbf{k}_1,\mathbf{k}_2}^{(-)*}(\mathbf{r}_1,\mathbf{r}_2)e^{i\mathbf{q}\cdot\mathbf{r}_2}\phi_0(\mathbf{r}_1,\mathbf{r}_2). \tag{9}$$

Note that M_0 would be zero if the initial and final two-electron states were exactly orthogonal. This is not the case for the wave functions we have used, but in practice the overlap integrals turn out to be rather small and the M_0 contribution to the T matrix is insignificant.

Quite a few models have been proposed to deal with two low-energy electrons in the continuum in an approximate way (see, e.g., [25]). We tested three of them in our previous studies for ion-impact induced DI [16] and consider them also here. The first and simplest one is a symmetrized product of one-electron scattering eigenstates $\phi_\mathbf{k}^{(-)}(\mathbf{r})$ of the bare helium nucleus with incoming boundary conditions. This wave function reads

$$\phi_{\mathbf{k}_1,\mathbf{k}_2}^{(-),2C}(\mathbf{r}_1,\mathbf{r}_2) = \frac{1}{\sqrt{2}}\left[\phi_{\mathbf{k}_1}^{(-)}(\mathbf{r}_1)\phi_{\mathbf{k}_2}^{(-)}(\mathbf{r}_2) + \phi_{\mathbf{k}_2}^{(-)}(\mathbf{r}_1)\phi_{\mathbf{k}_1}^{(-)}(\mathbf{r}_2)\right] \tag{10}$$

and is known as the 2-Coulomb (2C) model. It describes the two one-electron-nucleus subsystems exactly, but neglects the interaction between the electrons completely. The 2C model was used extensively in electron impact *single* ionization of helium [26] in order to describe the final state of the projectile

and the ejected electron. The absence of electron-electron correlations leads to an unphysical preference for both electrons to be found with similar momenta, a feature that was pointed out by several authors (see, e.g., [27] and references therein).

In the second and third models, we incorporate the electron-electron correlation in the final state in an approximate fashion. In both of them an attempt is made to fulfill the asymptotic boundary conditions of the three-body Coulomb problem, i.e., of the two ionized electrons and the residual target ion. More specifically, we use simplified versions of the so-called 3-Coulomb (3C) ansatz [28], in which the relative Coulomb scattering wave function of the two-electron subsystem is replaced by its value at zero spatial distance. The explicit expression for this wave function is [29]

$$\phi^{(-),2C+}_{\mathbf{k}_1,\mathbf{k}_2}(\mathbf{r}_1,\mathbf{r}_2) = \frac{1}{\sqrt{2}}\left[\phi^{(-)}_{\mathbf{k}_1}(\mathbf{r}_1)\phi^{(-)}_{\mathbf{k}_2}(\mathbf{r}_2) + \phi^{(-)}_{\mathbf{k}_2}(\mathbf{r}_1)\phi^{(-)}_{\mathbf{k}_1}(\mathbf{r}_2)\right]\alpha(k_{12}), \quad (11)$$

with

$$\alpha(k_{12}) = e^{-\pi\xi_{12}}\Gamma(1 - i\xi_{12}), \quad \xi_{12} = \frac{Z_{12}}{k_{12}}, \quad (12)$$

and $k_{12} = |\mathbf{k}_1 - \mathbf{k}_2|$ being the relative momentum between the two electrons. $Z_{12} = 1$ represents the case of *static screening*. Compared to the 2C model, the quantity

$$|\alpha(k_{12})|^2 = \frac{2\pi\xi_{12}}{e^{2\pi\xi_{12}} - 1} \quad (13)$$

known as the Gamow factor appears as a prefactor in the transition probabilities and cross sections. The Gamow factor suppresses exponentially the probability to find both ionized electrons with close momenta, but ensures that electrons with very different momenta move independently.

The choice $Z_{12} = 1$ yields too strong a repulsion between electrons with low emission energies, and consequently the cross sections near threshold are strongly underestimated. To remedy this flaw *dynamic screening* models were introduced. They are based on the idea of using effective charges that depend on the electron momenta [30–33]. Different explicit forms for this dependence have been discussed. Here we use a simple model proposed to describe $(e,3e)$ reactions [14] and further applied to model the correlation function in DI by ion impact [15]. It consists in using the effective charge

$$Z_{12} = 1 - \frac{k_{12}^2}{(k_1 + k_2)^2} \quad (14)$$

in Eq. (13). In our investigations of ion-induced DI we found that out of the three final-state models considered, the last one based on the effective charge (14) gives the most convincing results (see, e.g., [16]).

B. Higher-order mechanisms

A systematic account of the TS-2 mechanism involves the consideration of a second-order amplitude. On top of the inherent difficulties of such a calculation, this would require significantly more powerful computational resources than are currently available to us. Therefore, we content ourselves with a simulation of the TS-2 mechanism that makes use of the MCEG technique. The idea is to convolute two single-ionization (SI) events, which are both calculated in the FBA. The first SI step corresponds to the single ionization of the neutral helium atom by the incoming electron, while the second step is the ionization of the He^+ ion. The FDCS of each SI step is given by

$$\sigma_{\mathrm{SI,SI}^+} = \frac{d^5\sigma}{d\mathbf{k}d\mathbf{q}_\perp} \propto \left|T_{if}^{\mathrm{FBA}}\right|^2\delta(E_f - E_i), \quad (15)$$

where we have ignored the constants because they cancel out during the normalization procedure required by the MCEG. Within the FBA, the transition amplitude T_{if}^{FBA} can be written as

$$T_{if}^{\mathrm{FBA}} = \langle\chi_f^-|V_i|\chi_i^+\rangle, \quad (16)$$

where the initial (final) wave χ_i^+ (χ_f^-) is an approximation to the initial (final) state which satisfies outgoing-wave (+) [incoming-wave (−)] boundary conditions. The perturbation potential V_i in (16) is the Coulomb interaction between the projectile electron and the active target electron.

As in the case of the first-order model discussed in the previous section, the projectile electron is described in terms of plane waves. For the initial bound state, we employ a semianalytical Hartree-Fock-Roothaan wave function for the description of the neutral helium atom [34] and a hydrogenlike $1s$ state with $Z_T = 2$ for the He^+ ion. The final states of the ejected electrons are Coulomb waves with effective charges, namely, $Z_T = 1.69$ for the first ionization step in order to account for the partial screening of the nuclear charge and $Z_T = 2$ for the second step.

Another higher-order mechanism is TS-1-EL (for details about this model, see [17]). To calculate the FDCS using this approach we start with the same FBA amplitude that we employ for TS-1. The interaction of the projectile with the electron which was ejected through the electron-electron correlation is accounted for by convoluting the FDCS for TS-1 with classical elastic projectile-electron scattering using the MCEG technique. The projectile-target nucleus (PT) interaction also contributes to the various double-ionization channels. This interaction is not accounted for in the FBA amplitudes described in Secs. II A and II B.[1] In all our models (TS-1, TS-1-EL, and TS-2), it is incorporated retroactively by convoluting the FDCS with classical elastic scattering between the projectile electron and the target nucleus, also using the MCEG technique (for details, see [20]).

III. RESULTS AND DISCUSSION

In Fig. 1 the FDCS for double ionization of helium by 500 eV electron impact are shown for both electrons, each with an energy of 5 eV, ejected into the scattering plane defined by the initial and final projectile momenta as a function of the polar ejection angles of both electrons. The magnitude of the momentum transfer $\mathbf{q}$ is fixed at 0.8 a.u. Panel (a) shows our TS-1 calculation, in panel (b) the TS-1 results were convoluted with elastic projectile target nucleus scattering (TS-1-PT), and panels (c) and (d) show the TS-1-EL and TS-2

[1] If one disregards the insignificant but nonzero contribution of the overlap integral (7).

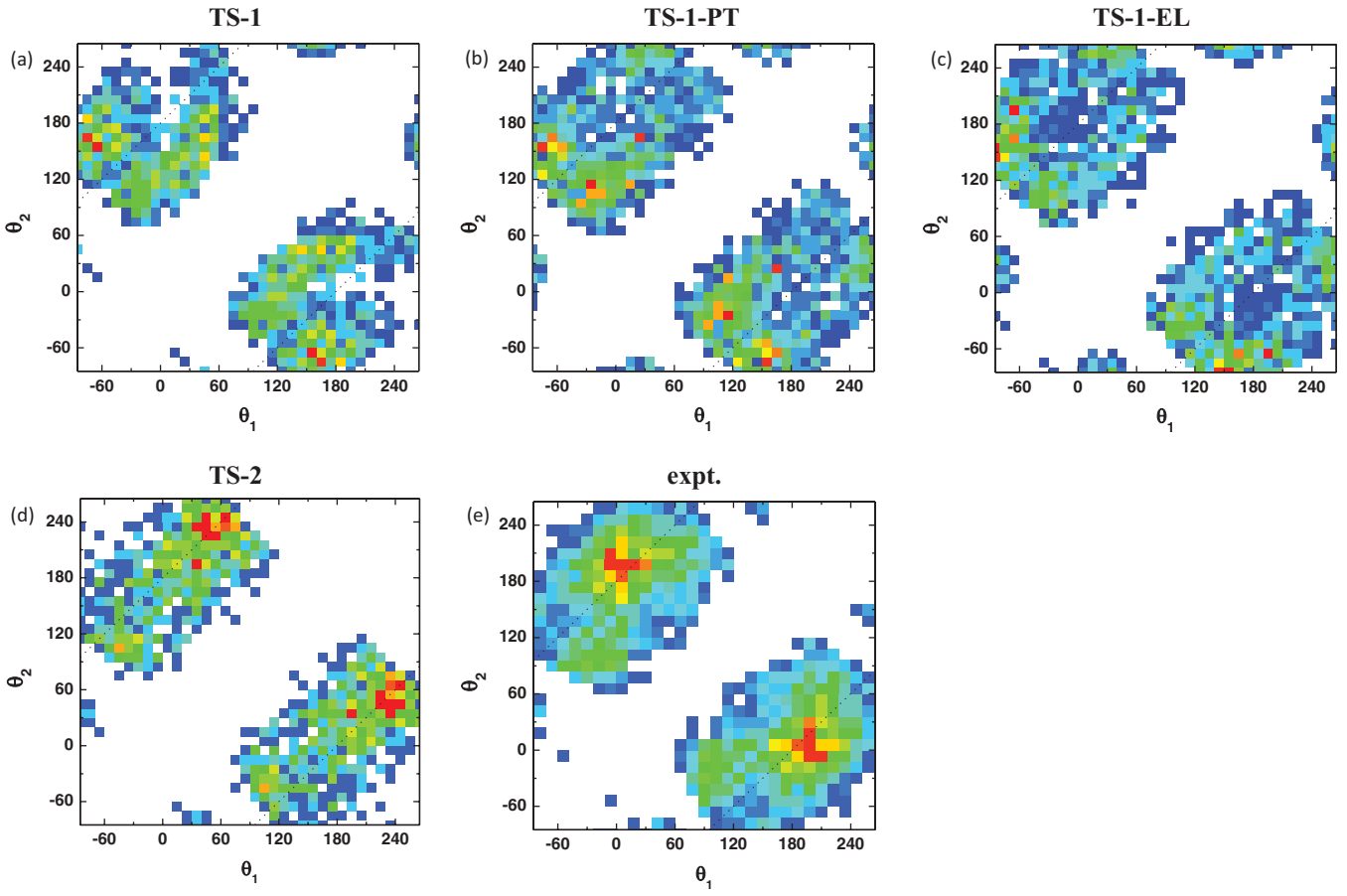

FIG. 1. (Color online) Fully differential cross section for double ionization of helium by 500 eV electron impact as a function of the polar emission angles (in degrees) of both electrons, each with an energy of 5 ± 2 eV, ejected into the scattering plane. The magnitude of the momentum transfer is fixed at $q = 0.8 \pm 0.2$ a.u. Panel (a) shows our TS-1 calculation, in panel (b) the TS-1 results were convoluted with elastic projectile target nucleus scattering (TS-1-PT), and panels (c) and (d) show the TS-1-EL and TS-2 results, respectively, also convoluted with PT scattering. Experimental data of Dorn *et al.* [6] are plotted in panel (e).

results, respectively, also convoluted with PT scattering. These calculations are compared to the experimental data of Dorn *et al.* [6] plotted in panel (e).

Generally, all variations of TS-1 calculations are in poor agreement with the experimental data. Particularly important are the discrepancies in the regions indicated by the dashed lines in Fig. 1, where the mutual angle between the two electrons is 180°. Electric dipole ($E1$) transitions cannot lead to such back-to-back emission of electrons with equal energy because of selection rules [29]. Indeed, in the TS-1 calculation, which is dominated by $E1$ transitions, a pronounced minimum along these lines can be seen. The convolution with elastic scattering of the projectile by either the target nucleus (TS-1-PT) or by one of the electrons (TS-1-EL) does not alter this minimum significantly. In contrast, in the experimental data, no systematic suppression of the FDCS along the $E1$-forbidden lines is observed. On the contrary, pronounced structures are observed at angle combinations of (0°,180°) and (180°,0°). This observation rules out the possibility that TS-1 in any variation is a major contributor to double ionization for these kinematic conditions.

Drastically improved qualitative agreement with experiment is obtained with our TS-2 calculation. Most notably, here we also find the main maxima in the FDCS at the $E1$-forbidden lines, although relative to the measured data they are shifted to larger angles for both electrons by about 30°. That TS-2 leads to maxima for back-to-back emission can be understood as follows: Because of angular momentum conservation and helicity considerations this process populates final two-electron states with angular momenta of 0 or 2, i.e., TS-2 cannot proceed through an $E1$ transition. Therefore, the Coulomb repulsion between the ejected electrons can now maximize the angle between them. Furthermore, a second pair of maxima at angle combinations of (−20°,100°) and (100°, − 20°) is well reproduced by the TS-2 calculation.

In Fig. 2 the same FDCS as in Fig. 1 are shown, except for the momentum transfer, which is now 2 a.u. The comparison between experiment and theory is very similar to the smaller momentum transfer. Here too, all variations of TS-1 calculations are in poor agreement with the measured data, which again exhibit pronounced maxima, rather than minima, at the $E1$-forbidden lines. On the other hand, the agreement with the TS-2 calculation is even improved compared to $q = 0.8$ a.u.. The position of the main maxima is now well reproduced. However, the second pair of maxima in the experimental data at (0,120°) and (120°,0) is somewhat shifted toward the $E1$-forbidden lines in the theoretical data. Nevertheless, the overall qualitative agreement between experiment and the

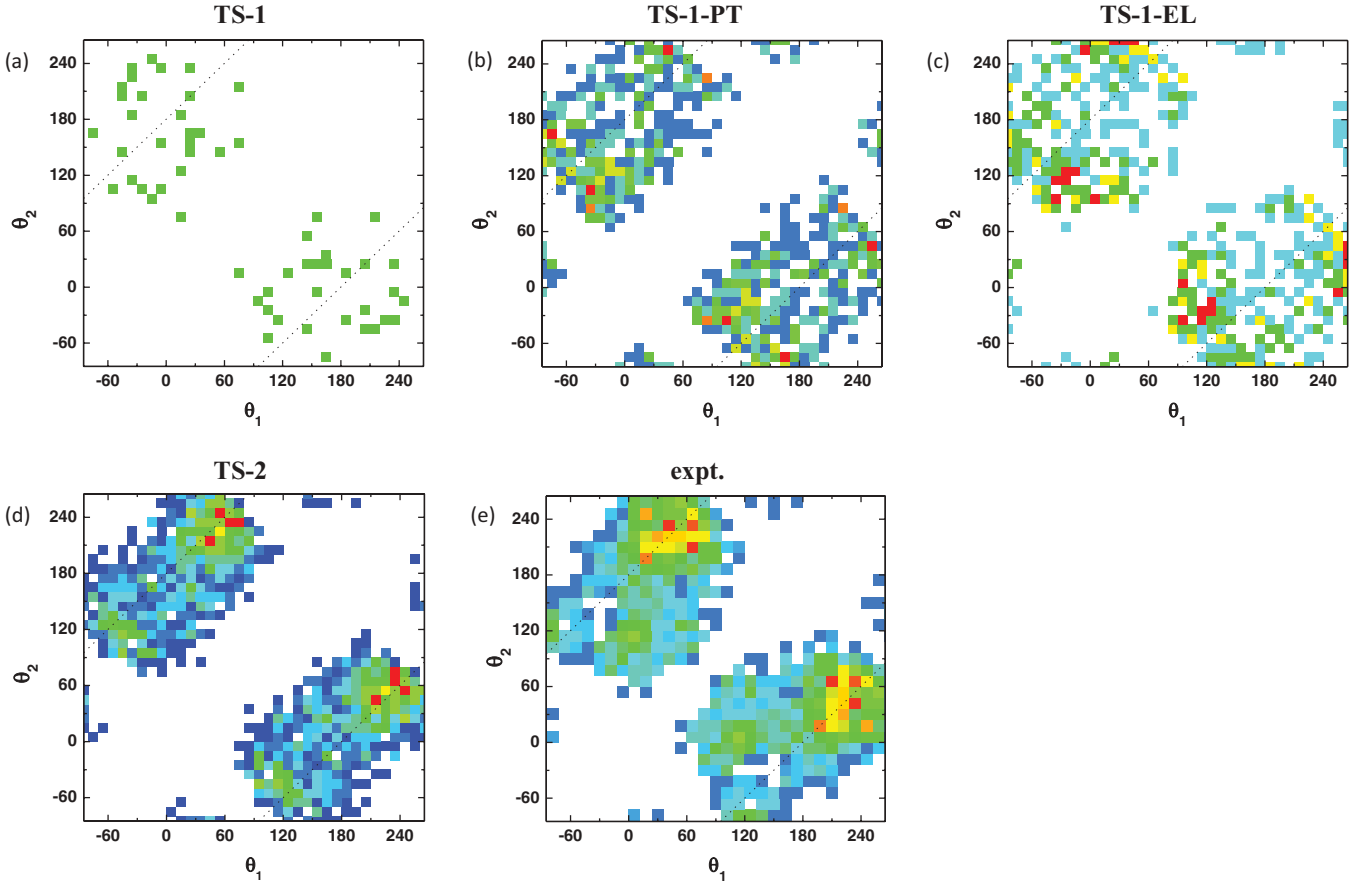

FIG. 2. (Color online) Same as Fig. 1, except $q = 2 \pm 0.3$ a.u.

TS-2 calculation is satisfactory and certainly much better than with all TS-1 based calculations. Our results thus strongly support the conclusions of Dorn *et al.* [6] and Lahmam-Bennani *et al.* [7,35,36] that double ionization is dominated by TS-2 down to relatively small η (0.165 in the present case).

To investigate to what extent the importance of TS-2 prevails at even smaller η we also compared our calculations to experimental data for an impact energy of 2 keV ($\eta = 0.08$) [5]. The FDCS for this energy are shown in Figs. 3 and 4 for $q = 0.6$ a.u. and ejected electron energies of 5 and 20 eV, respectively, for each electron. The panels show the calculations and the experimental data in the same order as Figs. 1 and 2. For both electron energies the TS-2 calculations still show pronounced maxima at the $E1$-forbidden lines, while in the experimental data a clear suppression of the FDCS along these lines is seen. Generally, the TS-2 calculations are in poor agreement with the measured cross sections. On the other hand, the calculations based on all variations of the TS-1 mechanism qualitatively reproduce the minima observed along the $E1$-forbidden lines.

The presence of the minima along the $E1$-forbidden lines in the experimental data and the comparison to theory demonstrates that at large projectile energies, double ionization proceeds predominantly through $E1$ transitions. However, this does not necessarily imply that higher-order contributions are unimportant. While a significant role of TS-2 can be ruled out at this large projectile energy, the variations of TS-1 involving elastic scattering of the projectile by the target nucleus or one of the electrons also represent higher-order mechanisms.

First, we discuss the role of elastic projectile-target nucleus scattering by comparing the TS-1 and TS-1-PT calculations to the measured data. The experimental FDCS show two pairs of maxima, one at angle combinations of about $(-10°,120°)$ and $(120°, -10°)$ and the second at about $(-5°,210°)$ and $(210°, -5°)$. For the former pair the momentum sum of both electrons points approximately in the direction of $\mathbf{q}$ and for the latter pair it is close to the direction of $-\mathbf{q}$. We therefore refer to these maxima as the binary peaks and recoil peaks, respectively, in analogy to standard notation in $(e,2e)$ studies. Both the positions and the shapes of the structures in the data are not reproduced very well by the TS-1 calculation for both ejected electron energies. In the position of the binary peaks the discrepancies are not too large; the measured position is only slightly shifted toward smaller angles. However, in the calculations the binary peaks are much more elongated than in the experiment. More importantly, the recoil peaks in the measured FDCS are shifted relative to the TS-1 calculation to larger angles by about 40° to 50°. This shift breaks the cylindrical symmetry of the angular distribution of the electron sum momentum about $\mathbf{q}$, which is strictly required for a first-order process. The shifted position of the recoil peak is thus a clear signature of significant higher-order contributions.

Including the PT interaction in the TS-1 model (TS-1-PT calculation) does lead to a shift of the binary peak to smaller

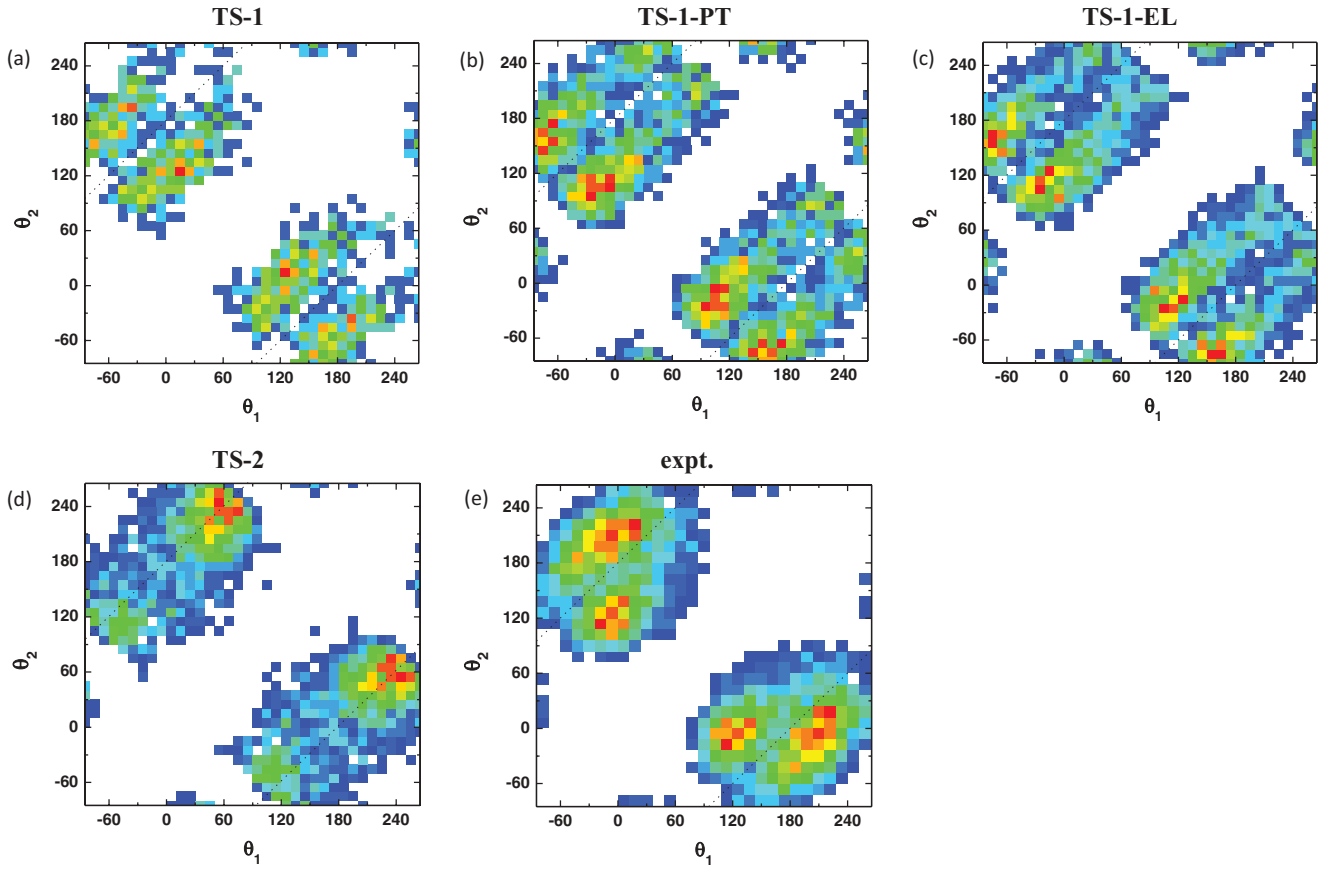

FIG. 3. (Color online) Same as Fig. 1, except incident electron energy is 2 keV and $q = 0.6 \pm 0.2$ a.u.

angles and also to some reduction in its elongation. However, this shift overshoots the experimental data, so that now the binary peak in the measured data is at too large angles. This could possibly be explained by an overestimation of the PT interaction. The convolution with elastic projectile-target nucleus scattering depends on the impact parameter range which mostly contributes to double ionization. The PT interaction tends to shift the binary peak to decreasing electron angles with decreasing impact parameters b. We estimated $bP(b)$, where $P(b)$ is the b-dependent double-ionization probability, based on the theoretical work of Foster *et al.* [11] on double ionization by fast proton impact for a similar η as studied here. However, there is no guarantee that $bP(b)$ is the same for proton and electron impact at equal speeds. Therefore, this estimate may introduce some uncertainties to the location of the binary peak.

A more serious problem with our model of incorporating the PT interaction is reflected by the observation that the recoil peak is shifted away from the experimental data so that the discrepancies already seen in the TS-1 results become even larger. The breaking of the cylindrical symmetry of the measured FDCS about **q**, associated with the large shift of the recoil peak compared to the TS-1 calculation, was not seen in similar data for double ionization by fast proton impact [8]. This difference in the cross sections for electron and ion impact can be explained by an interference between the various double-ionization mechanisms. In our model, cross sections, rather than amplitudes, are convoluted in order to incorporate the PT interaction. Therefore, any effect due to interference between amplitudes with and without the PT interaction cannot be reproduced, and this could explain the poor agreement of our calculations with experiment in the recoil peak.

In the case of double ionization by fast proton impact a clear manifestation of the PT interaction was found in four-particle Dalitz (4-D) plots [16,17], while its influence on the cross sections as a function of the ejection angles of the two electrons was found to be much weaker. For electron impact, experimental 4-D plots are not yet available. However, based on our studies on proton impact it seems very likely that for electron impact, too, effects due to the PT interaction would also be significantly more prominent in the 4-D plots than in the FDCS. It is quite possible that the PT interaction plays a less important role for electron impact, e.g., because larger impact parameters may contribute more strongly than for proton impact. However, for the latter the features in the 4-D plots caused by the PT interaction were so overwhelming that it is unlikely that the PT interaction is insignificant for electron impact. Furthermore, the shift of the binary peak and especially of the recoil peak relative to **q** is a clear signature of higher-order contributions, and those could involve the PT interaction. However, the comparison between the experimental and theoretical FDCS presented here is not conclusive with regard to the role of this interaction in double ionization by fast electron impact.

A comparison between our TS-1-PT and TS-1-EL calculations shows that in our model, elastic scattering between the

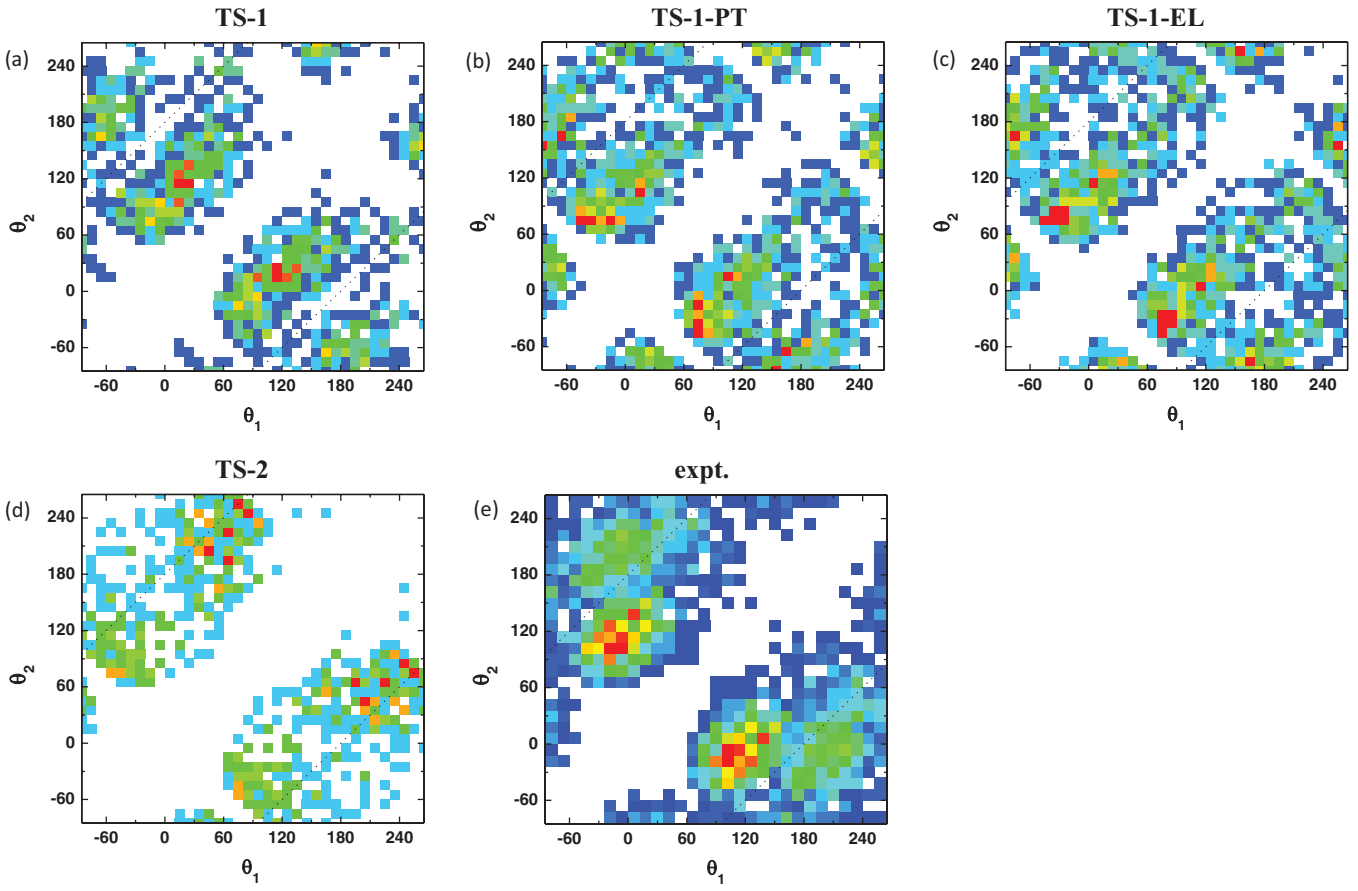

FIG. 4. (Color online) Same as Fig. 3, except the energy of each ejected electron is 20 ± 4 eV.

projectile and one of the ejected electrons has essentially no effect on the shape of the two-dimensional angular dependence of the FDCS. It should be noted, however, that especially at the smaller ejected electron energy, elastic scattering of the projectile by both the target nucleus and one of the electrons has a significant effect on the magnitude of the FDCS. At 5 eV the PT interaction increases the magnitude by about a factor of 2 compared to the TS-1 calculation and the elastic scattering by one of the electrons by an additional 30%. This increase reflects a broadening of the q dependence of the cross sections. This effect of elastic scattering of the projectile by the target nucleus and one of the electrons we also found in our calculations for proton impact, and it was confirmed by the experimental data [16,17]. Furthermore, once again we note that features due to elastic scattering from one electron, like the PT interaction, for proton impact were found to be much more prominent in the 4-D plots than in the two-dimensional angular dependence of the two electrons.

Although the comparison of the different variations of our TS-1 calculations with the experimental data does not enable us to conclusively evaluate the role of the PT interaction and the TS-1-EL process at 2 keV collision energy, the broken symmetry about **q** observed in the measured FDCS nevertheless clearly shows the importance of higher-order contributions. Such contributions were reported by Kheifets *et al.* at even larger projectile energies [37]. On the other hand, our TS-2 calculations demonstrate that this mechanism leads to maxima on top of the electric dipole forbidden lines, which are not observed in the measured data. This process can thus be ruled out as the dominant source of higher-order contributions. It seems likely that such contributions do involve the PT interaction and/or elastic scattering of the projectile from one electron, especially considering that the importance of these factors have been established already for proton impact at similar speed [17].

IV. CONCLUSIONS AND OUTLOOK

We have calculated contributions from various reaction mechanisms to double ionization of helium by electron impact. The data were compared to measured fully differential cross sections for equal ejected electron energies. Here, electric dipole ($E1$) selection rules prohibit back-to-back emission of the two electrons. Minima along the $E1$-forbidden lines were observed in the experimental data at a projectile energy of 2 keV, but at 500 eV pronounced maxima were found at these lines. For this last case, the data are well reproduced by our TS-2 calculations, especially for large momentum transfers, and poor agreement is obtained with all variations of TS-1 calculations. This leads us to conclude that at this energy, double ionization is dominated by TS-2, although the perturbation is relatively small ($\eta \approx 0.16$).

The pronounced suppression of back-to-back emission in the experimental data for 2 keV impact energy shows that, in contrast to 500 eV, $E1$ transitions are very important. At the same time the breaking of the symmetry about **q**,

observed in the data especially in the recoil peak, means that higher-order effects (other than TS-2 contributions) are significant as well. The suppression of back-to-back emission is reproduced by our TS-1 calculations. Furthermore, we demonstrated that including the projectile-target nucleus (PT) interaction in the TS-1 model does lead to a breaking of the symmetry about **q**. However, there are significant discrepancies in the position of the recoil peak to the data. Inclusion of elastic projectile-electron scattering has an effect on the magnitude of the FDCS; however, the shape of the two-dimensional angular dependence of the two electrons is hardly affected.

At a projectile energy of 500 eV our TS-2 model is in nice qualitative agreement with the experimental data. Earlier, we successfully applied a similar model to reproduce experimental 4-D plots obtained for ion impact at very large perturbation ($\eta = 5.83$) [18]. In that case, good agreement between experiment and theory was also achieved in two-dimensional angular distributions of the ejected electrons. This suggests that double ionization is dominated by TS-2 down to surprisingly small perturbations ($\eta \gtrsim 0.15$) and that our TS-2 model provides an adequate description of double ionization even for a relatively large projectile electron energy.

At very small perturbations ($\eta \lesssim 0.1$) the situation is less satisfactory. Here, the TS-2 model is, not surprisingly, in poor agreement with experimental data for both ion and electron impact. Measured data for proton impact are satisfactorily reproduced by our TS-1-EL calculations; however, the same model (or other variations of the TS-1 model) does not work very well for electron impact. We believe that this lack of success demonstrates the limitations of incorporating elastic scattering of the projectile by the target nucleus and one of the electrons classically in our model. Here, cross sections, rather than amplitudes, are convoluted. As a result, any interference between amplitudes with and without these elastic scattering components is not accounted for in our TS-1-EL model. On the other hand, indications were reported earlier that generally interferences between various transition amplitudes appear to be more important for electron impact than for ion impact [8].

ACKNOWLEDGMENTS

This work was supported by the National Science Foundation under Grant No. PHY0969299. T.K. acknowledges support from the Natural Sciences and Engineering Research Council of Canada.

[1] J. H. McGuire, *Electron Correlation Dynamics in Atomic Collisions* (Cambridge University Press, Cambridge, England, 1997).
[2] L. H. Andersen, P. Hvelplund, H. Knudsen, S. P. Møller, K. Elsener, K. G. Rensfelt, and E. Uggerhøj, Phys. Rev. Lett. **57**, 2147 (1986).
[3] R. Moshammer *et al.*, Phys. Rev. Lett. **77**, 1242 (1996).
[4] I. Taouil, A. Lahmam-Bennani, A. Duguet, and L. Avaldi, Phys. Rev. Lett. **81**, 4600 (1998).
[5] A. Dorn, A. Kheifets, C. D. Schröter, B. Najjari, C. Höhr, R. Moshammer, and J. Ullrich, Phys. Rev. Lett. **86**, 3755 (2001).
[6] A. Dorn, A. Kheifets, C. D. Schröter, C. Höhr, G. Sakhelashvili, R. Moshammer, J. Lower, and J. Ullrich, Phys. Rev. A **68**, 012715 (2003).
[7] A. Lahmam-Bennani, E. S. Casagrande, A. Naja, C. D. Cappello, and P. Bolognesi, J. Phys. B **43**, 105201 (2010).
[8] D. Fischer *et al.*, Phys. Rev. Lett. **90**, 243201 (2003).
[9] M. Schulz, R. Moshammer, W. Schmitt, H. Kollmus, B. Feuerstein, R. Mann, S. Hagmann, and J. Ullrich, Phys. Rev. Lett **84**, 863 (2000).
[10] S. Jones and D. H. Madison, Phys. Rev. Lett **91**, 073201 (2003).
[11] M. Foster, J. Colgan, and M. S. Pindzola, J. Phys. B **41**, 111002 (2008).
[12] X. Guan and K. Bartschat, Phys. Rev. Lett **103**, 213201 (2009).
[13] L. U. Ancarani, C. Dal Cappello, I. Charpentier, K. V. Rodríguez, and G. Gasaneo, Phys. Rev. A **78**, 062709 (2008).
[14] J. R. Götz, M. Walter, and J. S. Briggs, J. Phys. B **38**, 1569 (2005).
[15] L. Gulyás, A. Igarashi, and T. Kirchner, Phys. Rev. A **74**, 032713 (2006).
[16] M. F. Ciappina, M. Schulz, T. Kirchner, D. Fischer, R. Moshammer, and J. Ullrich, Phys. Rev. A **77**, 062706 (2008).
[17] M. Schulz, M. F. Ciappina, T. Kirchner, D. Fischer, R. Moshammer, and J. Ullrich, Phys. Rev. A **79**, 042708 (2009).
[18] D. Fischer *et al.*, Phys. Rev. A **80**, 062703 (2009).
[19] M. Dürr, B. Najjari, M. Schulz, A. Dorn, R. Moshammer, A. B. Voitkiv, and J. Ullrich, Phys. Rev. A **75**, 062708 (2007).
[20] M. Schulz, M. Dürr, B. Najjari, R. Moshammer, and J. Ullrich, Phys. Rev. A **76**, 032712 (2007).
[21] M. F. Ciappina, T. Kirchner, and M. Schulz, Comput. Phys. Commun. **181**, 813 (2010).
[22] M. Schulz, D. Fischer, T. Ferger, R. Moshammer, and J. Ullrich, J. Phys. B **40**, 3091 (2007).
[23] J. Berakdar, A. Lahmam-Bennani, and C. D. Cappello, Phys. Rep. **374**, 91 (2003).
[24] J. N. Silverman, O. Platas, and F. Matsen, J. Chem. Phys. **32**, 1402 (1960).
[25] L. G. Gerchikov and S. A. Sheinermann, J. Phys. B **34**, 647 (2001).
[26] C. DalCappello and H. LeRouzo, Phys. Rev. A **43**, 1395 (1991).
[27] B. Bapat *et al.*, J. Phys. B **32**, 1859 (1999).
[28] M. Brauner, J. S. Briggs, and H. Klar, J. Phys. B **22**, 2265 (1989).
[29] F. Maulbetsch and J. S. Briggs, J. Phys. B **26**, 1679 (1993).
[30] J. Berakdar and J. S. Briggs, Phys. Rev. Lett **72**, 3799 (1994).
[31] J. Berakdar, Phys. Rev. A **53**, 2314 (1996).
[32] J. Berakdar, Phys. Rev. A **54**, 1480 (1996).
[33] S. Zhang, J. Phys. B **33**, 3545 (2000).
[34] E. Clementi and C. Roetti, At. Data Nucl. Data Tables **14**, 177 (1974).
[35] A. Lahmam-Bennani, A. Duguet, and S. Roussin, J. Phys. B **35**, L59 (2002).
[36] A. Lahmam-Bennani, A. Duguet, C. Dal Cappello, H. Nebdi, and B. Piraux, Phys. Rev. A **67**, 010701(R) (2003).
[37] A. Kheifets, I. Bray, A. Duguet, A. Lahmam-Bennani, and I. Taouili, J. Phys. B **32**, 5047 (1999).